UDK 537.533:66.017:620.3
Professional article/Strokovni članek

ISSN 1580-2949
MTAEC9, 49(1)173(2015)

CHARACTERIZATION OF TiO_2 NANOPARTICLES WITH HIGH-RESOLUTION FEG SCANNING ELECTRON MICROSCOPY

KARAKTERIZACIJA NANODELCEV TiO_2 Z VISOKOLOČLJIVOSTNO FEG VRSTIČNO ELEKTRONSKO MIKROSKOPIJO

Zoran Samardžija[1], Domen Lapornik[2], Ksenija Gradišek[2], Dejan Verhovšek[2], Miran Čeh[1]

[1]Jožef Stefan Institute, Department for Nanostructured Materials, Jamova cesta 39, 1000 Ljubljana, Slovenia
[2]Cinkarna Celje, d. d., Metalurško-kemična industrija Celje, Kidričeva 26, 3001 Celje, Slovenia
zoran.samardzija@ijs.si

Prejem rokopisa – received: 2014-01-16; sprejem za objavo – accepted for publication: 2014-03-04

Ultrafine titanium dioxide powder (UF-TiO_2) has many applications as a result of its nanometer particle size and semiconducting electric properties. An upgraded method for synthesis of UF-TiO_2 was developed, with the ability to control the characteristics of the nanoparticles, i.e. their size, shape and crystal structure. In order to determine the correlation between the various synthesis parameters and the final form of the TiO_2 nanoparticles, their size and morphology were analyzed using high-resolution field-emission-gun scanning electron microscopy (FEGSEM). The UF-TiO_2 specimens for the FEGSEM high-magnification observations were prepared using three different routes. Micrographs were recorded with an inside-the-lens secondary electron detector and additionally using scanning transmission (STEM) mode. We found that coating the specimens with carbon or Au-Pd did not improve the image quality. Carbon coating was inappropriate because it filled the gaps between the nanoparticles giving the appearance of a smoothed, agglomerated surface. The TiO_2 nanoparticles sputtered with Au-Pd were observed to have better contrast; however, they were falsely enlarged due to the Au-Pd nano-layer around them. The best results were obtained with the uncoated specimens, where TiO_2 nanoparticles sized 5–10 nm were clearly visible at a magnification of 300 000-times. With STEM mode we were able to distinguish the TiO_2 nanoparticles relatively easily; however with different image contrast than when using standard SEM mode.

Keywords: titanium dioxide, nanoparticles, FEGSEM

Prah titanovega dioksida z nanodelci (UF-TiO_2) ima vsestranske aplikacije, ki izhajajo iz majhne velikosti delcev in njegovih polprevodniških električnih lastnosti. Nadgrajena je bila metoda za sintezo UF-TiO_2 z možnostjo kontrole lastnosti nanodelcev: njihove velikosti, oblike in kristalne strukture. Za določanje vpliva različnih parametrov sinteze na končno obliko nanodelcev TiO_2 je bila preiskovana njihova velikost in oblika z visokoločljivostnim vrstičnim elektronskim mikroskopom s katodo na poljsko emisijo (FEGSEM). Vzorci UF-TiO_2 so bili pripravljeni za analize FEGSEM na tri različne načine. Posnetki so bili narejeni z detektorjem sekundarnih elektronov, nameščenim v objektni leči mikroskopa in dodatno v presevnem načinu (STEM). Ugotovljeno je, da prevodne plasti ogljika ali Au-Pd, ki so bile nanesene na površino vzorcev, ne izboljšajo kakovosti slike. Nanos amorfne plasti ogljika je bil neprimeren, ker je zapolnil prostor med nanodelci, dajajoč vtis zglajene, aglomerirane površine. Nanodelci v vzorcu, ki je bil napršen z Au-Pd, so bili vidni z boljšim kontrastom, vendar so bili navidezno večji, kot so v resnici, zaradi dodane plasti Au-Pd okoli njih. Najboljši rezultati so bili dobljeni z opazovanjem nenapršenega vzorca, kjer so bili osnovni nanodelci TiO_2 z velikostjo od 5 nm do 10 nm jasno vidni pri 300 000-kratni povečavi. S STEM je relativno enostavno razločiti nanodelce TiO_2, vendar z drugačnim slikovnim kontrastom v primerjavi s standardnim SEM-načinom.

Ključne besede: titanov dioksid, nanodelci, FEGSEM

1 INTRODUCTION

Ultrafine, nanometer-grade titanium dioxide (UF-TiO_2) is known for its versatile applications, originating from its very high specific surface due to the nano-sized particles and its semiconducting electric properties. The range of use for TiO_2 nanoparticles in its two crystalline forms, anatase or rutile, is very wide: photocatalytic applications, UV absorbing transparent coatings, plastics additive, cosmetics UV blockers, photo-electrochromic windows, DSSCs ("dye-sensitized solar cells") and many more.[1–3] The production of TiO_2 material with a high specific surface is one of the core development activities in the factory Cinkarna Celje, with a strategic orientation towards the production of UF-TiO_2 in water-suspension form. For that reason the gel-sol synthesis method was employed and upgraded to obtain anatase and/or rutile TiO_2 nanoparticles.[4] To study the influence of various reaction parameters of the gel-sol synthesis on the characteristics of the final UF-TiO_2 product it is necessary to perform fast and reliable analyses of the samples of TiO_2 powders that consist of nanoparticles. Namely, it is necessary to have reliable data on the particle size and the morphology of the ultrafine powders after each synthesis protocol in order to establish the correct correlation between the processing parameters and the material's characteristics according to a specific application. A modern field-emission-gun scanning electron microscope (FEGSEM) with a very-high-brightness cathode is one of the analytical tools that can be used for the characterization of nanoparticles. The very small, focused, electron-probe diameter in the FEGSEM makes it possible to observe the specimens with an ultimate resolution of about 1 nm.[5] In this work we implemented

advanced methods of FEGSEM microscopy to study the ultrafine, nano-sized TiO_2 powders and to determine the morphology and the size of both the agglomerates and the constituent TiO_2 nanoparticles.

2 EXPERIMENTAL

For the FEGSEM analyses the powder specimens with ultrafine TiO_2 nanoparticles were prepared in three different ways. Initially, the TiO_2 nanoparticles were dispersed from properly diluted suspensions using an ultrasonic device and then deposited and dried on polished aluminum holders. The first-type specimens were uncoated, the second-type specimens were coated with an amorphous carbon layer 4 nm and the third-type specimens were coated with a layer 3 nm of Au-Pd alloy. The coatings were applied in a Gatan PECS 682 ion-beam coating apparatus with specimen rotation up to 20 r/min, tilt up to 25° and a rocking speed of 10° s^{-1}. The specimens were observed using two FEGSEM microscopes: a JEOL JSM-7600F and a Zeiss Sigma VP. The FEGSEM experimental set-ups were adjusted and optimized according to the individual specimen and the desired final magnification, with an emphasis on the preferential application of low-voltage high-resolution microscopy.[6] Thus the applied SEM accelerating voltages were set in the range 2–10 kV with electron-beam currents of 20–100 pA and working distances of 3–10 mm. An inside-the-lens secondary-electron detector was used for the imaging. All the images were recorded without noise-reduction tools. In addition, the SEM scanning-transmission (STEM) mode was used at 30 kV with samples that were prepared by the direct dispersion of the nanoparticles on a thin carbon-membrane.

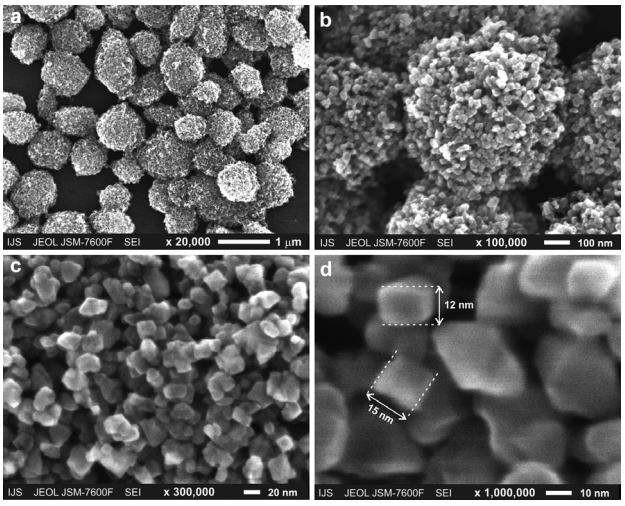

Figure 1: FEGSEM micrographs of the ultrafine anatase TiO_2: a) submicrometer-sized agglomerates of the nanoparticles, b), c) basic anatase nanoparticles in the agglomerates at 100 000-times and 300 000-times magnifications, d) the image of the anatase nanocrystallites at highest accessible 1 000 000-times magnification

Slika 1: FEGSEM-posnetki zelo finega prahu anatasa TiO_2: a) submikrometrsko veliki aglomerati nanodelcev, b), c) osnovni nanodelci anatasa v aglomeratih, posneti pri povečavah 100 000-krat in 300 000-krat, d) posnetek nanokristalitov anatasa pri največji možni povečavi 1 000 000-krat

3 RESULTS AND DISCUSSION

The high-resolution FEGSEM micrographs of the uncoated specimen of the ultra-fine TiO_2 anatase powder were recorded using a sequence of magnifications, as shown in **Figure 1**. The rounded agglomerates of the particles with a size of ≤ 1 μm remained stable, even after applied ultrasonic dispersion, as displayed in **Figure 1a**. The micrographs at higher magnifications of 100 000-times and 300 000-times (**Figures 1b** and **1c**) clearly revealed, angularly shaped, constituent anatase nanocrystallites within the agglomerates. From these images the size of the crystallites was easily estimated to be up to 20 nm. Furthermore, exploiting the limits of the microscope by operating under specially optimized imaging conditions, we were able to record the images of the basic nanocrystallites at an ultimate, maximum magnification of 1 000 000-times, as presented in **Figure 1d**. Dimensional measurements were then performed directly on the image and these confirmed that the size of the anatase nanocrystallites is in the range 10–20 nm. Moreover, the shape of some nanocrystallites was recognized as being similar to octahedra, which is typical for the anatase crystal structure.[7]

Two samples of crystalline UF-TiO_2, rutile and anatase, were prepared employing identical sample preparation routes and then examined using the same FEGSEM set-up with a final magnification of 100 000-times. The micrograph presented in **Figure 2** shows rutile nanoparticles in the form of "wheat-like" grains with a size of 20–40 nm, also exhibiting a narrow size distribution as a consequence of the inherent monodispersed nature of the rutile precursor within the applied synthesis procedure.[8] In contrast, the anatase sample looks different, revealing the presence of nano-agglomerates that consisted of very small, basic nanoparticles with a size

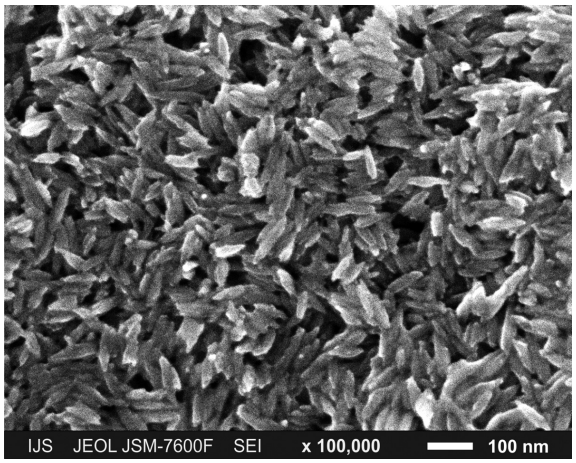

Figure 2: The micrograph of the basic nanoparticles of rutile UF-TiO_2

Slika 2: Posnetek osnovnih nanodelcev UF-TiO_2 rutila

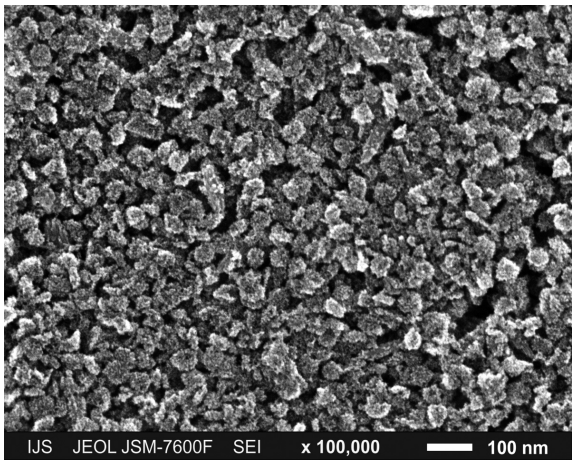

Figure 3: The micrograph of nanometer-sized agglomerates of anatase UF-TiO_2

Slika 3: Posnetek aglomeratov nanodelcev UF-TiO_2 anatasa

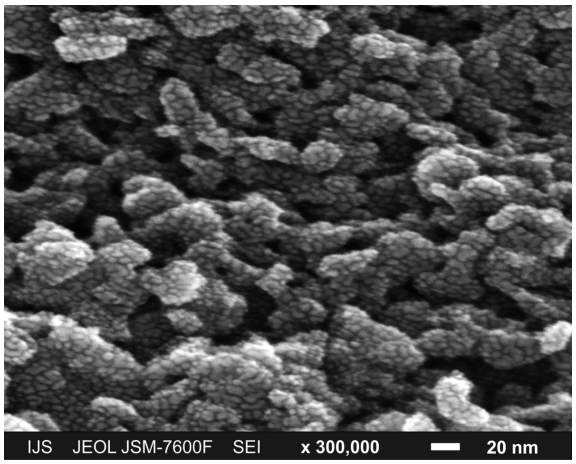

Figure 5: The high-resolution micrograph of the details of nanometer-sized anatase agglomerates; specimen coated with Au-Pd layer

Slika 5: Visokoločljivostni posnetek detajla nanometrskih aglomeratov anatasa; vzorec, napršen s plastjo iz zlitine Au-Pd

below 10 nm, as shown in **Figure 3**. The size of these agglomerates was between 20 nm and 40 nm only.

In order to get a more detailed view of the constituent anatase nanoparticles the specimens were additionally treated using the three preparation routes mentioned in the experimental part. An ultra-high-magnification 300 000-times micrograph of the uncoated anatase specimen is shown in **Figure 4** and clearly reveals the authentic structure of the nano-agglomerates, which consist of the basic TiO_2 nanoparticles sized 5–10 nm. In the case of the uncoated sample, surface charging was avoided by operating at a properly selected accelerating voltage, with lower beam currents and using faster scanning speeds for the recording. A similar image of the specimen coated with a Au-Pd nanolayer shown in **Figure 5** provides basically the same information as given in **Figure 4**; however, due to applied coating the agglomerates seem somewhat rounded and also the nanoparticles are falsely slightly larger. The imaging of the Au-Pd-coated anatase specimen was easier to perform than for the uncoated specimen, because the sample was more stable under the electron-beam and was sufficiently conductive to avoid charging artifacts, thus allowing us to operate at higher beam currents. Also, the image contrast and signal-to-noise ratio were better using higher currents and because of the high secondary-electron yield of the Au-Pd material. If one would neglect these artificial changes to the morphology due to the Au-Pd coating, these prepared samples are acceptable, especially because of the easier FEGSEM high-magnification imaging. In comparison with the uncoated and the Au-Pd-coated samples the third anatase sample that was coated with carbon appeared very different, as shown in **Figure 6**. An amorphous carbon layer covered the surface of the agglomerates, filling the gaps between the nanoparticles. Therefore, the agglomerates look

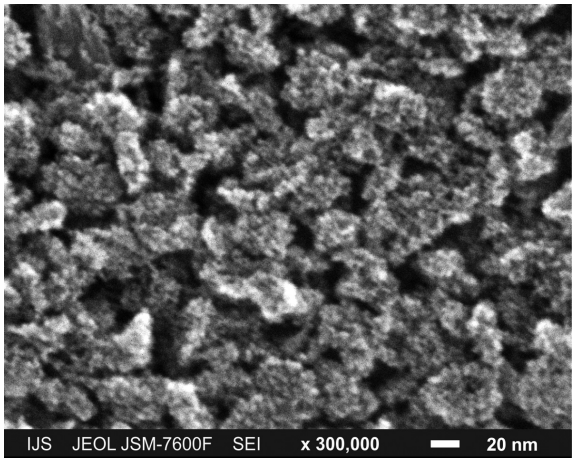

Figure 4: The high-resolution micrograph of the details of nanometer-sized anatase agglomerates with constituent TiO_2 nanoparticles sized 5–10 nm; uncoated specimen

Slika 4: Visokoločljivostni posnetek detajlov nanometrskih aglomeratov anatasa z osnovnimi nanodelci TiO_2 z velikostjo 5–10 nm; nenapršen vzorec

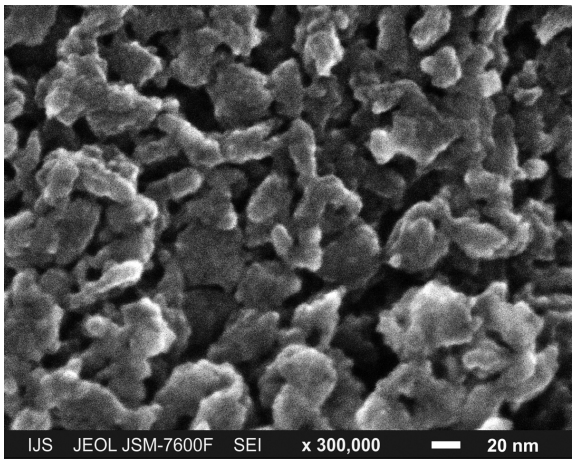

Figure 6: The high-resolution micrograph of nanometer-sized anatase agglomerates; specimen coated with amorphous carbon layer

Slika 6: Visokoločljivostni posnetek nanometrskih aglomeratov anatasa; vzorec, napršen z amorfno plastjo ogljika

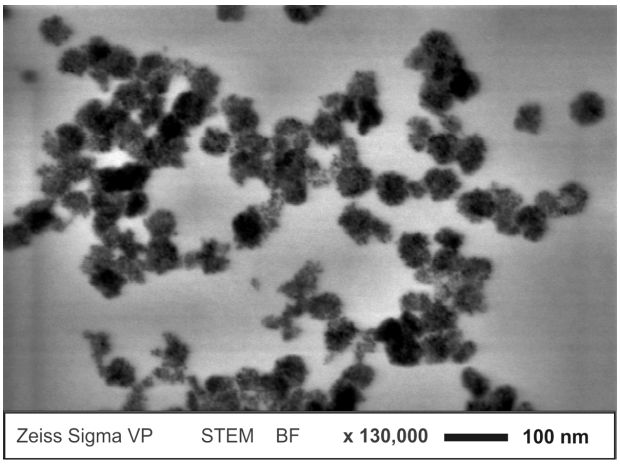

Figure 7: STEM bright-field image of nanometer-sized anatase agglomerates
Slika 7: STEM-posnetek v svetlem polju nanometrskih aglomeratov anatasa

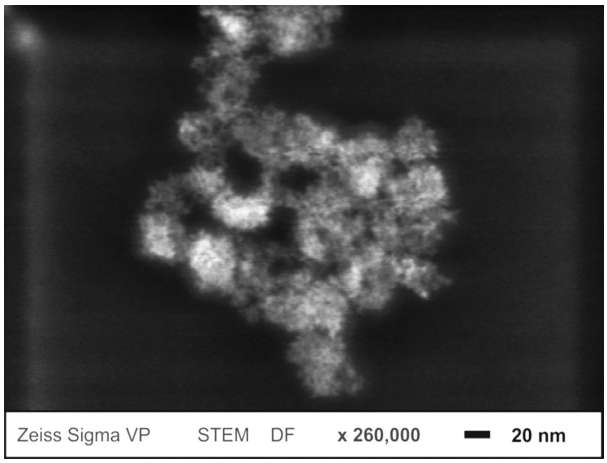

Figure 8: STEM dark-field image of nanometer-sized anatase agglomerates and nanoparticles
Slika 8: STEM-posnetek v temnem polju nanometrskih aglomeratov in nanodelcev anatasa

falsely smooth and in this case it was not possible to resolve the basic TiO_2 nanoparticles.

A complementary bright-field (BF) STEM image of agglomerated anatase nanoparticles is presented in **Figure 7**. Because of the high applied accelerating voltage (30 kV) the issues related to accurate astigmatism correction and precise electron-beam centering are less pronounced, although they are very important in the standard imaging mode. The contours of the agglomerates are sharp and visible, thus allowing a straightforward estimation of their size. The drawback of the STEM observation is rapid sample contamination and the subsequent loss of image contrast. Once the area of interest is found, the STEM images have to be recorded as quickly as possible so as to reduce the contamination and to keep the image contrast at the desired level. The basic anatase nanoparticles were also visible in STEM mode. In this case dark-field (DF) imaging was used at higher magnifications, as shown in **Figure 8**. The bright spot in the upper-left corner of the image and the visible traces of the grey frame arise from the contamination that occurred within several seconds of exposure under the electron-beam.

4 CONCLUSIONS

The morphology, size and size distribution of the ultrafine titanium dioxide powders consisting of nanoparticles were successfully analyzed using a high-resolution FEGSEM with useful images attained at magnifications up to 1 000 000-times. By comparing the images of the differently prepared samples we found that sputtered conductive layers of either carbon or Au-Pd do not improve the quality of the FEGSEM micrographs. The best micrographs were obtained on genuine, uncoated specimens where TiO_2 nanoparticles sized 5–10 nm were clearly revealed at a 300 000-times magnification. Carbon coating was found to be inappropriate because it filled the gaps between the nanoparticles, making the agglomerates artificially smooth. The nanoparticles in the specimen coated with Au-Pd could be observed easily with better contrast; however, they appeared slightly bigger because of the coating. Using the STEM mode we were able to see agglomerated anatase nanoparticles relatively easily, albeit with a different image contrast. The best images for the characterization of the morphology and the size of TiO_2 nanoparticles were recorded using the inside-the-lens secondary electron detector and the appropriate FEGSEM set-ups optimized for ultra-high-magnification observation.

Acknowledgements

This work was supported by the Slovenian Research Agency (ARRS) within the project J2-4237 "Electron microscopy and microanalysis of materials on submicrometer scale".

5 REFERENCES

[1] Z. Zhang, C. C. Wang, R. Zakaria, J. Y. Ying, J. Phys. Chem. B, 102 (**1998**), 10871–10878
[2] A. L. Linsebigler, G. Lu, J. T. Yates Jr., Chem. Rev., 95 (**1995**), 735–758
[3] B. O'Regan, M. Gratzel, Nature, 353 (**1991**), 737–740
[4] T. Sugimoto, X. Zhou, A. Muramatsu, J. Colloid Interface Sci., 259 (**2003**), 43–52
[5] J. I. Goldstein, D. E. Newbury, D. C. Joy, C. E. Lyman, P. Echlin, E. Lifshin, L. Sawyer, J. R. Michael, Scanning Electron Microscopy and X-Ray Microanalysis, 3rd ed., Kluwer Academic Publishers, New York 2003, 34
[6] S. Asahina, T. Togashi, O. Terasaki, S. Takami, T. Adschiri, M. Shibata, N. Erdman, Microscopy and Analysis, 26 (**2012**), S12–S14
[7] Y. Li, T. J. White, S. H. Lim, J. Solid State Chem., 177 (**2004**), 1372–1381
[8] J. Park, V. Priman, E. Matijević, J. Phys. Chem. B, 105 (**2001**), 11630–11635